arXiv:astro-ph/0106182v1 11 Jun 2001

Propagation of UHECRs from the Sources in the Super-Galactic Plane

Yoshinori Ide[1], Shigehiro Nagataki[1], Sinya Tsubaki[1],

Hiroyuki Yoshiguchi[1] and Katsuhiko Sato[1,2]

[1]Department of Physics, School of Science, the University of Tokyo, 7-3-1 Hongo, Bunkyoku, Tokyo 113-0033, Japan

[2]Research Center for the Early Universe, School of Science, the University of Tokyo, 7-3-1 Hongo, Bunkyoku, Tokyo 113-0033, Japan

Received _____; accepted _____

ABSTRACT

We have performed the detailed numerical simulations on the propagation of the UHE protons in the energy range $E = (10^{19.5} - 10^{22.0})$ eV in the relatively strong extra-galactic magnetic field with strength $B = (10, 100)$ nG within about 40 Mpc. In this case, the deflection angles of UHECRs become so large that the no counterparts problem is simply solved. As for the source distribution, we assumed that it is proportional to the number distribution of galaxies within the GZK sphere. We have found many clusters, which mean the small-scale anisotropy, in our simulations. It has been also shown that the observed energy spectrum is well reproduced in our models without any fine-tuned parameter. We have used the correlation value in order to investigate statistically the similarity between the distribution of arrival directions of UHECRs and that of galaxies. We have found that each correlation value for each parameter set begins to converge when the number of the detected events becomes $O(10^3)$. Since the expected number counts by the experiment of the next generation such as TA, HiRes, Auger, and EUSO are thought to be the order of 10^3, we will be able to determine the source distribution and values of the parameters in this study in the very near future. Compared with the AGASA data, the significant anisotropy on the arrival directions of UHECRs are found in the analysis of first and second harmonics. This may originate from the incompleteness of the ORS database. This problem may be also solved if the source distribution is slightly changed. For example, this problem may be solved if we assume that UHECRs come from some of the galaxies such as AGNs and radio galaxies.

Subject headings: cosmic rays — methods: numerical — ISM: magnetic fields — galaxies: general — large-scale structure of universe

1. INTRODUCTION

The observed differential cosmic ray spectrum is remarkably featureless and extends beyond 10^{20} eV (Takeda et al. 1999). So far, the observed number of the Ultra High Energy Cosmic Rays (hereafter UHECRs) whose energies are above 10^{20} eV (this is the definition of UHECRs in this study) is only 25 (Virmani et al. 2000). On the other hand, a new generation of the ground-based large aperture experiments such as Telescope Array (hereafter TA; Telescope Array Project Design Report 2000), HiRes (Wilkinson et al. 1999) and South and North Auger (Capelle et al. 1998) is expected to detect about 1000 UHECRs until 2010 (Zas 2001). Moreover, the mission proposed as EUSO is devoted to the exploration of UHECRs from satellites and is expected to detect about 1000 UHECRs per year (Bhattacharjee and Sigl 1998). We will be able to discuss statistically the feature of UHECRs, such as arrival direction, in the very near future.

The mechanism to produce such highly energetic cosmic rays is still controversial. In most of the conventional acceleration scenarios, which are called bottom-up scenarios, effects of diffusive shock acceleration are taken into consideration (e.g., Biermann 1995; Halzen and Zas 1997; Waxman 2000). So far, by using Hillas-plot (Hillas 1984; Selvon 2000), gamma-ray bursts (GRBs) and/or active galactic nuclei (AGN) are considered as probable candidates. On the other hand, there is a large number of production models based on exotic particle physics scenarios (see Bhattacharjee and Sigl 2000 and references therein). Sometimes effects of interaction or collapse of Topological Defects are taken into consideration to produce such massive exotic particles (e.g., Bhattacharjee et al. 1992). These scenarios are called top-down scenarios. In this study, we mainly consider bottom-up scenarios although top-down scenarios are very attractive and important. This is because top-down scenarios are highly model-dependent and observational constraints on them are

little at present. Thus we investigate in this study whether the present observations on UHECRs can be explained by bottom-up scenarios or not.

In the bottom-up scenarios, charged particles are accelerated due to Fermi acceleration mechanism and obey a power law spectrum (Fermi 1949). However, the large distances between the Earth and potential UHECRs sources like GRBs and AGNs lead to another problem called GZK effect (Greisen 1966; Zatsepin and Kuz'min 1966). As for the protons, the energy at which the GZK cutoff takes place ($\sim 7 \times 10^{19}$ eV) is given by the threshold for photopion production in the collisions of protons and CMB photons. It is reported that the loss length ($l_{\rm loss} = Edl/dE$) falls below 13 Mpc above 100 EeV (Stanev et al. 2000). As for nuclei, the situation is considered to be worse due to the photo-disintegration mechanism (Stanev et al. 2000). Thus we assume in this study that the composition of UHECRs is proton.

Taking the GZK sphere for protons into consideration, we can easily understand the difficulty of the situation, that is, no plausible source counterparts within the GZK sphere have been found within a few degrees from the arrival directions of UHECRs, which are considered to be the typical deflection angles of UHECRs (e.g., Blasi and Olinto 1998). Moreover, there is a puzzling problem on the distribution of the arrival directions of UHECRs (e.g., Blasi and Olinto 1998). It is reported that there is no significant large-scale anisotropy of arrival direction distribution of UHECRs. On the other hand, there are one triplet and three doublets within a separation angle of 2.5 degrees for the 47 cosmic rays above 4×10^{19} eV, and the probability of observing these clusters by a chance coincidence under an isotropic distribution is smaller than 1% (Takeda et al. 1999). We have to give a natural explanation for these puzzling problems.

In this paper, we propose a bottom-up scenario in which the sources of UHECRs are correlated with the Super-Galactic Plane (SGP). This is because the probability of

observing the clusters by a chance coincidence under such a distribution becomes relatively large ($\sim$ 10 %) (Lemoine et al. 1999). In fact, we show in this study that such clusters emerge very frequently in our model. It is also shown that the observed energy spectrum is well reproduced in our models without any fine-tuned parameter. Moreover, we show statistically that the correlation between the arrival directions of UHECRs and SGP can not be determined significantly at the present number of data (25 enevts), which is consistent with the AGASA data (Takeda et al. 1999). We conclude that about 1000 events, which are attained in the very near future as mentioned above, are necessary to determine whether the source distribution is correlated with SGP or not. Moreover, we introduce a relatively large amplitude of the extra-galactic magnetic field ($\sim$ 10 nG) in order to solve the no counterpart problem. This is our picture for solving the problems on UHECRs.

In this study, images of arrival directions of UHECRs are simulated. Optical Redshift Survey (ORS) data (Santiago et al. 1995) is used as the source distribution of UHECRs. Such a realistic data has not been used in the simulation of propagation of UHECRs in the previous works. Inhomogeneity of the arrival directions of UHECRs are also discussed statistically by introducing the correlation value, which has not been introduced in the previous works (e.g. Lemoine et al. 1999). These are new points of this work. We also show one realization of arrival directions of UHECRs above 4×10^{19} eV in order to compare our results with the AGASA data (Takeda et al. 1999). First and second harmonics analysis for our model is also presented in order to compare directly our results with the AGASA data (Takeda et al. 1999). Our conclusion has been already stated above.

In section 2, we show our method of calculation. Results are shown in section 3. Summary and discussion are presented in section 4.

2. METHOD OF CALCULATION

2.1. Method of Calculation for Propagation of UHECRs

In this subsection, we describe the method of Monte Carlo simulations for the propagation of UHECRs. At first, we assume that the composition of UHECRs is proton. We also assume that the initial energy spectrum of the UHECRs obeys the power-law, that is, $dN/dE \propto E^{-2}$, where N denotes the number of UHECRs. Initial energies of UHECRs are assumed to be in the range of $(10^{19.5}$ – $10^{22})$eV. The number of injected UHECRs in a simulation is 10^6 except for the cases of $l_c = 1$Mpc, where l_c is the correlation length of the extra-magnetic field and is explained below. In the case of (B, l_c) = (10nG, 1Mpc), the number of the injected particles is 10^5, where B is the strength of the extra-magnetic field and is explained below. In the case of (B, l_c) = (100nG, 1Mpc), the number of injected particles is 2.5×10^4.

As for the energy loss processes, electron-positron pair creation and photopion production in the CMB field are included. Particles below $\sim 10^{19.5}$ eV lose their energies mainly by pair creations and above it lose their energies mainly by photopion production (Yoshida and Teshima 1993). We adopt the formulation of the energy loss rate for the pair production on isotropic photons, which has been shown by Chododowski et al. (1992) According to them, the energy loss rate of a relativistic nucleus for the pair production on isotropic photons is given by

$$-\frac{d\gamma}{dt} = \alpha r_0^2 c Z^2 \frac{m_e}{m_A} \int_2^\infty d\kappa n\left(\frac{\kappa}{2\gamma}\right) \frac{\varphi(\kappa)}{\kappa^2}, \tag{1}$$

where γ is the Lorenz factor of the particle, $\kappa = 2k\gamma$ (k is the momentum of the particle in units of $m_e c$), $n(\kappa)$, α, r_0, Z, and m_A are the photon distribution in the momentum space, the fine-structure constant, the classical electron radius, the charge of the particle, and the rest mass of the particle, respectively. For the energy range $E \geq 10^{19.0}$ eV, φ can

be represented well as

$$\varphi \to \kappa \sum_{i=0}^{3} d_i \ln^i \kappa, \tag{2}$$

$$d_0 \simeq -86.07,\ d_1 \simeq 50.96,\ d_2 \simeq -14.45,\ d_3 = 8/3. \tag{3}$$

We also adopt the formulation of the energy loss rate for the photopion production on isotropic photons, which has been shown by Achterberg et al. (1999). According to them, the interaction length of the photopion production, $l_{p\gamma}(E_p)$, in the CMB can be written as

$$l_{p\gamma}(E_p)/\mathrm{Mpc} \simeq \begin{cases} 0.9 \left(\frac{E_p}{E_\mathrm{b}}\right)^2 e^{E_\mathrm{b}/E_p}, & \text{for} \quad E_p \leq 0.2E_\mathrm{b} \\ 4.8, & \text{for} \quad E_p > 0.2E_\mathrm{b} \end{cases}, \tag{4}$$

where E_p is the proton energy in the cosmic rest frame and E_b is defined as

$$E_\mathrm{b} \equiv \frac{m_p \varepsilon_\mathrm{th}}{2k_\mathrm{b}T} \left(= E_p \frac{\varepsilon_\mathrm{th}}{2\gamma_p k_\mathrm{b} T} \right). \tag{5}$$

Here $\varepsilon_\mathrm{th} \equiv m_\pi(1 + m_\pi/2m_p) \simeq 145\mathrm{MeV}$ is the threshold energy of photon in the proton rest frame. As for the mean inelasticity, it can be written as

$$K_p \equiv \frac{E_t^2 + m_\pi^2 - m_p^2}{2E_t^2}, \tag{6}$$

where E_t is defined as

$$E_t = \sqrt{m_p^2 + 2m_p\varepsilon_0}. \tag{7}$$

Here ε_0 is the photon energy in the proton rest frame. As for the maximum spread of inelasticity from the mean one, it can be written as

$$K' \equiv \frac{\sqrt{(E_t^2 - m_+^2)(E_t^2 - m_-^2)}}{2E_t^2} \tag{8}$$

$$= \sqrt{(K_P + K_+)(K_P - K_-)}, \tag{9}$$

where $m_\pm \equiv m_p \pm m_\pi$ and $K_\pm \equiv m_\pi/(m_p \mp m_\pi)$. Since photopion productions obey the Poisson statistics, we can calculate the energy losses of UHECRs by the photopion production using the formulations mentioned above.

Next, the details on the extra-magnetic field, which is little known theoretically and observationally, is described. Its strength and detailed structure are not known, although the strength of the magnetic field in the local super cluster is thought to be relatively strong. Only its observational upper limit, $\sim 1\mu$G in the meaning of r.m.s., has been obtained from the Faraday rotation of the distant sources (Ryu and Biermann 1998). In this study, 10 nG and 100nG are adopted as the r.m.s. of the magnetic field. They seems to be strong to be sure (Sigl et al. 1998). However, such strong magnetic field is required to solve the problem that there seems to be no plausible source counterparts within the GZK sphere within a few degrees from the arrival directions of UHECRs. We also assume that the magnetic field is represented as the Gaussian random field with zero mean and a power-law spectrum. Thus, $\langle B^2(k)\rangle$ can be written as

$$\langle B^2(k)\rangle \propto k^{n_H} \quad \text{for} \quad k \leq k_{\rm cut} \tag{10}$$

$$= 0 \qquad \text{otherwise,} \tag{11}$$

where $k_{\rm cut} = 2\pi/l_{\rm cut} = 16\pi/l_{\rm c}$ characterizes the numerical cut-off scale that is explained below and n_H is chosen to be -11/3 so as to represent the Kolmogorov spectrum. As for the wave numbers of the magnetic field, 8 discrete ones are introduced in this study. In practice, $k_i = 0, \pm k_0, \pm 2k_0, \pm 3k_0, 4k_0$ are used as wave numbers. Here k_0 is $2\pi/l_c$. As for the correlation length of the magnetic field, l_c, three different values are adopted in this study. They are 1 Mpc, 10 Mpc, and 40 Mpc. 1 Mpc is widely used as the typical value of the correlation length of the extra-galactic magnetic field. 10 Mpc and 40 Mpc represent the scale hight and the scale length of the local super cluster, respectively. We separate one cubic cell of the size l_c into 512 ($= 8^3$) smaller cells of the size $l_c/8$, which corresponds to $l_{\rm cut}$ mentioned above. The magnetic field are assigned to each small cell. As for the boundary condition, the periodic boundary condition is adopted in order to reduce storage data for magnetic field components.

Finally, we explain the source distribution of UHECRs. In this study, we assume that the distribution of sources of UHECRs is proportional to that of the galaxies within the GZK sphere. In practice, we use the realistic data from the Optical Redshift Survey (ORS; Santiago et al. 1995). It is noted that the source distribution will be such like that when GRBs occur very frequently in every galaxies. It is also noted that the source distribution may be such like that in the top-down scenarios, too. This is because the sources of UHECRs such as massive exotic particles will be trapped in the gravitational potential of galaxies and/or clusters of galaxies. As for the dependence of our conclusion presented in this study on the source distribution, we will report it in the forthcoming paper.

2.2. Statistics on the Arrival Directions of UHECRs

2.2.1. Method of Calculation of Correlation Value

In this study, we introduce the correlation value in order to investigate statistically the similarity between the distribution of arrival directions of UHECRs and that of galaxies within the GZK sphere. The correlation value, Ξ, between two distributions f_i and f_s, is defined as

$$\Xi(f_i, f_s) \equiv \frac{\rho(f_i, f_s)}{\sqrt{\rho(f_i, f_i)\rho(f_s, f_s)}}, \tag{12}$$

where

$$\rho(f_a, f_b) \equiv \sum_{j,k} \left(\frac{f_a(j,k) - \bar{f}_a}{\bar{f}_a} \right) \left(\frac{f_b(j,k) - \bar{f}_b}{\bar{f}_b} \right) \frac{\Delta\Omega(j,k)}{4\pi}. \tag{13}$$

Here subscripts j and k discriminate each cell of the sky, $\Delta\Omega(j,k)$ denotes the solid angle of the (j,k) cell, and $\bar{f}$ means the average of f. In this study, the size of the cell is chosen to be $1^\circ \times 1^\circ$. The meaning of Ξ is as follows. By definition, Ξ ranges from -1 to $+1$. When $\Xi = +1$, two distributions are same exactly. When $\Xi =$ -1, two distributions are exactly

opposite. When $\Xi = 0$, we can not find any resemblance between two distributions.

Strictly speaking, the angular images obtained by numerical simulations do not mean the exact distributions of the UHECRs which we will detect indeed, but the probability density distributions for the arrival directions of UHECRs. Thus, in order to investigate the correlation between the results of numerical simulations and the distribution of galaxies in the ORS catalogue statistically, we have to make a lot of data samples for the arrival directions of UHECRs assuming the numerically obtained probability density distribution. In order to estimate the effects of selecting the events stochastically, the number of data samples is set to be 1000 for the same number of events of UHECRs, N, under the same condition (e.g., B and l_c). Hence, a mean value and a standard deviation of Ξs can be obtained for each N and condition.

In practice, we choose the 6 different values for the number (N) of events of UHECRs. These are 25, 10^2, 320, 10^3, 3200, and 10^4. 25 is the present number of events of UHECRs (Virmani et al. 2000). Other values are chosen arbitrarily only paying attention to the fact that the expected number counts detected by the experiment of the next generation such as TA, HiRes, Auger, and EUSO are thought to be the order of 10^3 (Bhattacharjee and Sigl 1998).

2.2.2. Analysis of First and Second Harmonics

In order to search for the global anisotropy in the arrival directions of UHECRs, we apply harmonics analysis to the galactic longitude distribution of events (Hayashida et al. 1999). It should be noted that we do not investigate the right ascension distribution but investigate the galactic longitude distribution so as not to suffer from the problem of the

incompleteness of the ORS catalog, which does not contain any data within $|b| \leq 20^\circ$ (see Figure 5). We will explain the definition of it below (see Hayashida et al. 1999 in detail). The m-th harmonic amplitude, r, and phase of maximum, θ, are obtained for a sample of n measurements of phase, ϕ_1, ϕ_2, $\cdots$, ϕ_n $(0 \leq \phi_i \leq 2\pi)$ from:

$$r = (a^2 + b^2)^{1/2} \tag{14}$$

$$\theta = \tan^{-1}(b/a) \tag{15}$$

where, $a = \frac{2}{n}\Sigma_{i=1}^{n} \cos m\phi_i$, $b = \frac{2}{n}\Sigma_{i=1}^{n} \sin m\phi_i$.

The following k represents the statistical significance. If events with total number n are uniformly distributed in galactic longitude, the chance probability of observing the amplitude $\geq r$ is given by,

$$P = \exp(-k), \tag{16}$$

where

$$k = nr^2/4. \tag{17}$$

We take n to be 47 in the range $E \geq 4 \times 10^{19}$eV in order to compare our results with AGASA data (Takeda et al. 1999), although the right ascension distribution of events are investigated in their harmonics analysis. We also take n to be 100 in each energy bin in the range $10^{19.15} \leq E \leq 10^{19.5}$eV. However, it is noted that the results of harmonic analysis for the energy range $E \leq 10^{19.5}$eV may not be reliable. This is because the initial energy of UHECRs is restricted to be in the range of $10^{19.5} \leq E \leq 10^{22}$eV to save the CPU time.

3. RESULTS

3.1. Arrival Directions and Energy Spectra of UHECRs

In this subsection, we show the images of the distribution of the arrival directions of UHECRs. We note again that the resolution of the image, that is, the size of the cell is taken to be $1^\circ \times 1^\circ$. It is also noted that these images show the probability density distributions of arrival directions of UHECRs. The observed distribution should be interpreted as one realization. That is why we have to discuss the correlation among them statistically. In the following subsections, the statistical discussion is presented.

At first, in the left panel of Figure 1, the distribution of the galaxies within 40 Mpc in ORS data catalogue is shown. In the right panel of Figure 1, the image in the case of $B = 10$ nG, $l_c = 10$ Mpc, $H_0 = 75$ km/s/Mpc, and $E \geq 10^{19.5}$ eV is shown. The inter-contour interval is 0.5 in the logarithm to base 10 of the integral flux per solid angle. We can find that the image is distorted due to the deflection caused by extra-galactic magnetic field.

Next, the parameter dependence of these images is investigated. In the left panel of Figure 2, the image in the same case with Figure 1b but for $E \geq 10^{20.0}$ eV is shown. We find that the image in Figure 2a is more sharp and similar to the image of the distribution of galaxies than that in Figure 1b. It is easily understood because more energetic charged CRs propagates more straightly. In the right panel of Figure 2, the image in the same case with Figure 2a but for $B = 100$ nG is shown. Even for the energetic UHECRs, the deflection angle becomes relatively large and the image is much distorted as long as the amplitude of the extra-galactic magnetic field is taken to be large (~ 100 nG).

The dependence of these images on the correlation length, l_c, is shown in Figure 3. In the left panel of Figure 3, the image in the same case with Figure 2a but for $l_c = 1$ Mpc is shown. On the other hand, in the right panel of Figure 3, the image in the same case with Figure 2a but for $l_c = 40$ Mpc is shown. As is shown in Figure 3, the effect of l_c on the deflection is relatively weak. This is because the deflection angle is proportional to B and $l_c^{1/2}$, respectively.

EDITOR: PLACE FIGURE 1 HERE.

EDITOR: PLACE FIGURE 2 HERE.

EDITOR: PLACE FIGURE 3 HERE.

In Figure 4, we show one realization of arrival directions of UHECRs above 4×10^{19} eV in equatorial coordinates for the case of $B = 10$nG and $l_c = 1$Mpc. For comparison, we show the distribution of the galaxies within 40 Mpc in ORS data catalogue in equatorial coordinates in Figure 5. In Figure 4, the number of events is chosen to be 47 in order to compare our results with the AGASA data (Takeda et al. 1999). The arrival directions of UHECRs are restricted in the range $-15^\circ \leq b \leq 80^\circ$ in order to compare our results with the AGASA data. Clusters which mean the small-scale anisotropy of UHECRs can be found clearly. This result suggests that the probability of observing these clusters is relatively high in our model. This is consistent with the conclusion presented by Lemoine et al. (1999). In fact, we show in Figure 6 the distribution of the neighbor event (sr^{-1}) as a function of the separation angle between the two events whose energies are above 4×10^{19} eV. It can be written as

$$N(\theta) = \frac{1}{2\pi|\cos\theta - \cos(\theta + \delta\theta)|} \sum_{\theta \leq \phi \leq \theta + \delta\theta} 1 \quad [\mathrm{sr}^{-1}], \tag{18}$$

where ϕ denotes the separation angle of the two events. $\delta\theta$ is taken to be 5° in this analysis. The number of events in a data sample is chosen to be 47. The number of data samples is set to be 1000 in order to obtain the mean value in every bin. We can find clearly the significant peak at samll separation angles, which indicates the small-scale anisotropy of UHECRs. We also show in Figure 7 the event number of clusters such as doublets and

triplets within a separation angle of 2.5° in a data sample which contains 47 events, whose energies are above 4×10^{19} eV. The number of data samples is set to be 20 in order to obtain the mean values. We can find that the average number of clusters such as doublets and triplets is consistent with the AGASA data (Takeda et al. 1999).

EDITOR: PLACE FIGURE 4 HERE.

EDITOR: PLACE FIGURE 5 HERE.

EDITOR: PLACE FIGURE 6 HERE.

EDITOR: PLACE FIGURE 7 HERE.

Finally, the calculated energy spectra of UHECRs are shown in Figure 8. The parameters are set to be $B = 10$ nG and $H_0 = 75$ km/s/Mpc. The cases of $l_c = 1$, 10 and 40 Mpc are shown respectively. The energy spectra are normalized to the AGASA data (Takeda et al. 1999) at $E = 100$ EeV. We think that the observed energy spectrum is well reproduced by all the cases in Figure 8 without any fine-tuned parameter.

EDITOR: PLACE FIGURE 8 HERE.

3.2. Correlation Value

In this subsection, we discuss statistically the correlation between the distribution of galaxies within GZK sphere and arrival directions of UHECRs.

At first, correlation values defined in subsection 2.2.1 are shown in Figure 9 for the case of $B = 10$ nG, $l_c = 10$ Mpc and $H_0 = 75.0$ km/s/Mpc indicating the influence of the selected energy range. In this figure, $n = 0$, $n = 1$, and $n = 2$ denote $E \geq 10^{19.5}$eV, $E \geq 10^{20.0}$eV, and $E \geq 10^{21.0}$eV, respectively. It should be emphasized that the present observed number (N) of UHECRs of order 10^1 is too small to estimate the final correlation values. When N is close to the order of 10^3 – 10^4, the correlation values begin to converge and final correlation values can be estimated. It is well confirmed in Figure 10, in which each Ξ is normalized by its final value. We emphasize again that a new generation of the ground-based large aperture experiments is expected to detect about 1000 UHECRs until 2010 (Zas 2001). Moreover, the mission EUSO is expected to detect about 1000 UHECRs per year (Bhattacharjee and Sigl 1998). So we will be able to determine the source distribution in the very near future.

EDITOR: PLACE FIGURE 9 HERE.

EDITOR: PLACE FIGURE 10 HERE.

In Figure 11, the correlation values are shown in the case of $H_0 = 75$ km/s/Mpc and $E \geq 10^{20}$ eV indicating the influence of B and l_c. It is confirmed again that the influence of B is greater than l_c, which is indicated in the previous subsection. Furthermore, we can find again that the number of UHECRs of order 10^3 is required to estimate the final correlation value.

EDITOR: PLACE FIGURE 11 HERE.

3.3. First and Second Harmonics

We show the results of the first (left panel) and second harmonics (right panel) in the galactic longitude in Figure 12, 13, and 14. The amplitudes, phases, and chance probability of harmonics are shown in these figures. The parameters are set to be $B = 10$nG and $l_c = 1$Mpc. The number of data, n, in one data sample is chosen to be 47 in the energy range (4×10^{19} – 2×10^{20} eV) in order to compare our results with the AGASA data (Takeda et al. 1999). The number of data samples is set to be 1000 in order to obtain the mean value and the standard deviation in every bin.

Compared with the AGASA data, the significant anisotropy on the arrival directions of UHECRs can be seen. This may originate from the fact that the results of harmonic analysis for the energy range $E \leq 10^{19.5}$eV are not correct. This is because the initial energy of UHECRs is restricted to be in the range of $10^{19.5} \leq E \leq 10^{22}$eV to save the CPU time. This may also originate from the incompleteness of the ORS database. That is, this database does not contain any data within $|b| \leq 20^\circ$ (see Figure 5). Also, this problem may be solved if the source distribution is slightly changed. For example, this problem may be solved if we assume that UHECRs come from some of the galaxies such as AGNs and radio galaxies. We will investigate in detail the dependence of our conclusion presented in this study on the source distribution in the forthcoming paper.

4. SUMMARY AND DISCUSSION

We have performed the detailed numerical simulations on the propagation of the UHE protons in the energy range $E = (10^{19.5} - 10^{22.0})$ eV in the relatively strong extra-galactic

magnetic field with strength $B = (10, 100)$ nG within about 40 Mpc. In this case, the deflection angles of UHECRs become so large that the no counterparts problem is simply solved.

We have made the images of the angular distribution of UHECRs assuming that the source distribution is proportional to the density distribution of matter, or the galaxy distribution of the ORS data calatog within 40 Mpc. It is noted that the images obtained by numerical simulations do not mean the exact distributions of the UHECRs which we will detect indeed, but the probability density distributions for the arrival directions of UHECRs. We have found that the influence of l_c on these images are very weak, while that of B is very strong.

We have found many clusters, which mean the small-scale anisotropy, in our simulations. This is the advantage to assume that the source distribution is not isotropic. It has been also shown that the observed energy spectrum is well reproduced in our models without any fine-tuned parameter.

We have used the correlation value Ξ in order to investigate statistically the similarity between the distribution of arrival directions of UHECRs and that of galaxies within the GZK sphere. We have found that the values of the parameters are indistinguishable at the level of the present number of the events, 25. Also, we have found that we are not still able to determine whether the source distribution of UHECRs is correlated with the SGP or not.

When the number of the detected events becomes $O(10^3)$, the correlation values for each parameter set begins to separate and converge. Thus, when the experimental data accumulate in the near future, the estimation for the values of parameters will be possible by the analysis of the correlation values. The expected number counts by the experiment of the next generation such as TA, HiRes, Auger, and EUSO are thought to be the order of 10^3 (Bhattacharjee and Sigl 1998). Thus, we will be able to determine the source distribution

and values of the parameters in this study in the very near future.

Compared with the AGASA data (Takeda et al. 1999), the significant anisotropy on the arrival directions of UHECRs can be seen in the analysis of first and second harmonics. This may originate from the fact that the results of harmonic analysis for the energy range $E \leq 10^{19.5}$eV are not correct. This is because the initial energy of UHECRs is restricted to be in the range of $10^{19.5} \leq E \leq 10^{22}$eV to save the CPU time. This may also originate from the incompleteness of the ORS database. That is, this database does not contain any data within $|b| \leq 20^{\circ}$. Also, this problem may be solved if the source distribution is slightly changed. For example, this problem may be solved if we assume that UHECRs come from some of the galaxies such as AGNs and radio galaxies. We will investigate in detail the dependence of our conclusion presented in this study on the source distribution in the forthcoming paper.

This research has been supported in part by a Grant-in-Aid for the Center-of-Excellence (COE) Research (07CE2002) and for the Scientific Research Fund (199908802) of the Ministry of Education, Science, Sports and Culture in Japan and by Japan Society for the Promotion of Science Postdoctoral Fellowships for Research Abroad.

REFERENCES

Achterberg A., Gallant Y., Norman C.A., Melrose D.B. 1999, astro-ph/9907060

Bhattacharjee P., Hill C.T., Schramm D.N. 1992, PRL, 69, 567

Bhattacharjee P., Sigl G. 1998, astro-ph/9811011

Bhattacharjee P., Sigl G. 2000, Phys. Rep. 327, 109

Biermann P.L. 1995, PRD, 51, 3450

Blasi P., Olinto V. 1998, PRD, 59, 023001

Capelle K.S., Cronin J.W., Parente G., Zas E. 1998, APh, 8, 321

Chodorowski M.J., Zdziarske A.A., Sikora M. 1992, ApJ, 400, 181

Fermi E. 1949, Phys. Rev., 75, 1169

Greisen K., PRL, 1966, PRL, 16, 748

Halzen F., Zas E. 1997, ApJ, 488, 669

Hayashida N., et al. 1999 APh, 10, 303

Hillas A.M. 1984, Ann. Rev. Astron. Astrophys., 22, 425

Lemoine M., Sigl G., Biermann P. 1999, astro-ph/9903124

Ryu D., Biermann P.L., 1998, A&A, 335, 19

Santiago B.X., Strauss M.A., Lahav O., Davis M., Dressler A., Huchra J.P. 1995, ApJ, 446, 457

Selvon A.L. 2000, astro-ph/0009444

Sigl G., Lemoine M., Biermann P. 1998, astro-ph/9806283

Stanev et al. 2000, astro-ph/0003484

Takeda M., et al. 1999, ApJ, 522, 225

Telescope Array Project Design Report 2000, http://www-ta.icrr.u-tokyo.ac.jp

Virmani A., Bhattacharya S., Jain P., Razzaque S., Ralston J.P. and McKay E.W. 2000, astro-ph/0010235

Waxman E. 2000, Nucl. Phys. Proc. Suppl., 87, 345

Wilkinson C.R., et al. 1999, APh, 12, 121

Yoshida S., Teshima M. 1993, Prog. Theor. Phys. 89, 833

Zas E. 2001, astro-ph/0103371

Zatsepin G.T., Kuz'min V.A. 1966, JETP Lett., 4, 78

This manuscript was prepared with the AAS LaTeX macros v4.0.

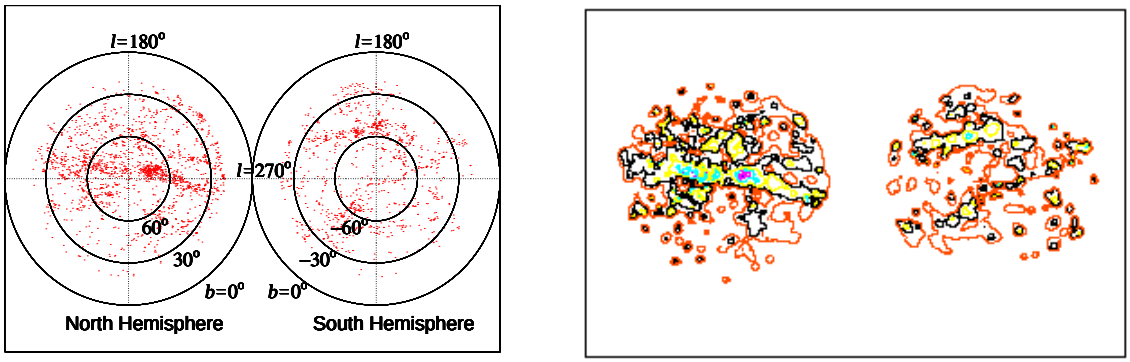

Fig. 1.— (a) left panel: angular distribution of galaxies in Optical Redshift Survey (ORS) data within 40Mpc. (b) right panel: distribution of arrival directions of UHECRs in the case of $B = 10$ nG, $l_c = 10$ Mpc, $H_0 = 75$ km/s/Mpc, and $E \geq 10^{19.5}$ eV. Galactic coordinate is used and left parts correspond to the north galactic hemisphere. The resolution of the image is set to be $1^\circ \times 1^\circ$. The inter-contour interval is 0.5 in the logarithm to base 10 of the integral flux per solid angle.

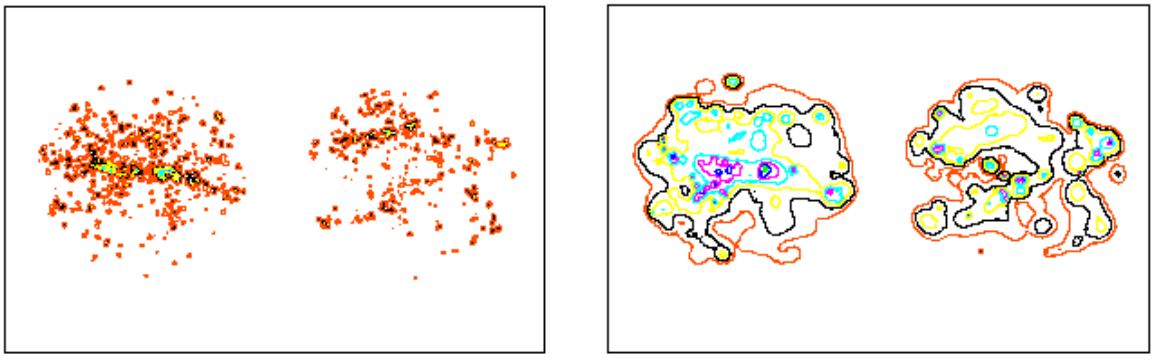

Fig. 2.— (a) left panel: Same with Figure 1b, but for $E \geq 10^{20.0}$ eV. (b) right panel: Same with Figure 2a, but for $B = 100$ nG.

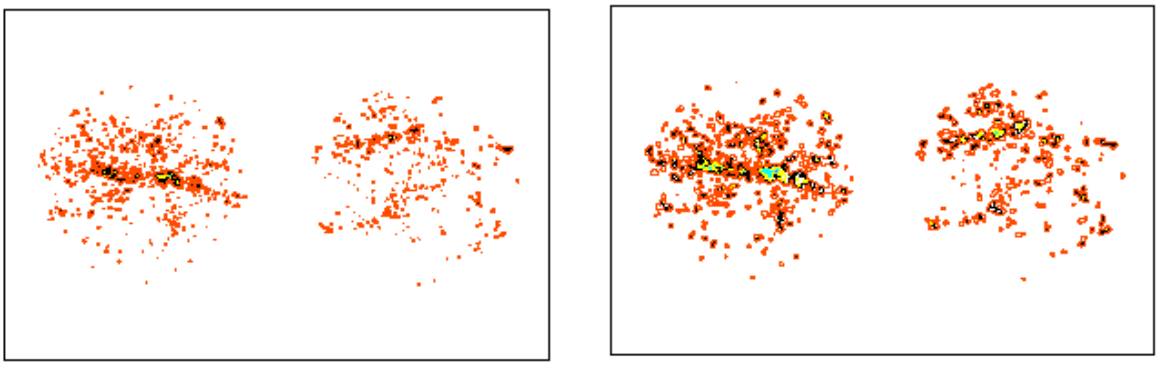

Fig. 3.— (a) left panel: Same with Figure 2a, but for $l_c = 1$ Mpc (b) right panel: Same with Figure 2a, but for $l_c = 40$ Mpc

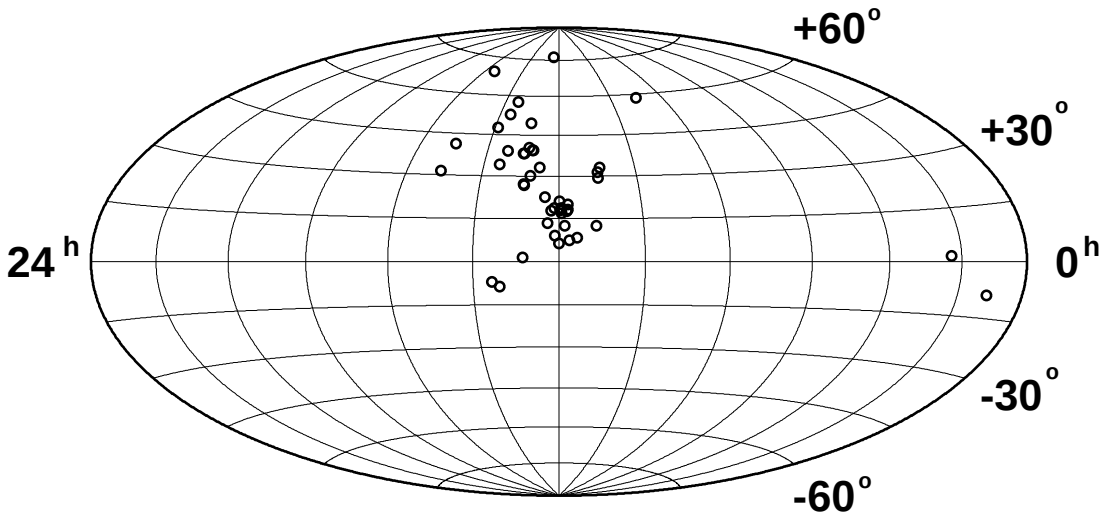

Fig. 4.— Arrival directions of UHECRs above 4×10^{19} eV in equatorial coordinates for the case of $B = 10$nG and $l_c = 1$Mpc. The number of events is chosen to be 47 in order to compare our results with the AGASA data (Hayashida 1999). The arrival directions of UHECRs are restricted in the range $-15^\circ \leq b \leq 80^\circ$ in order to compare our results with the AGASA data. Clusters which mean the small-scale anisotropy of UHECRs can be found clearly.

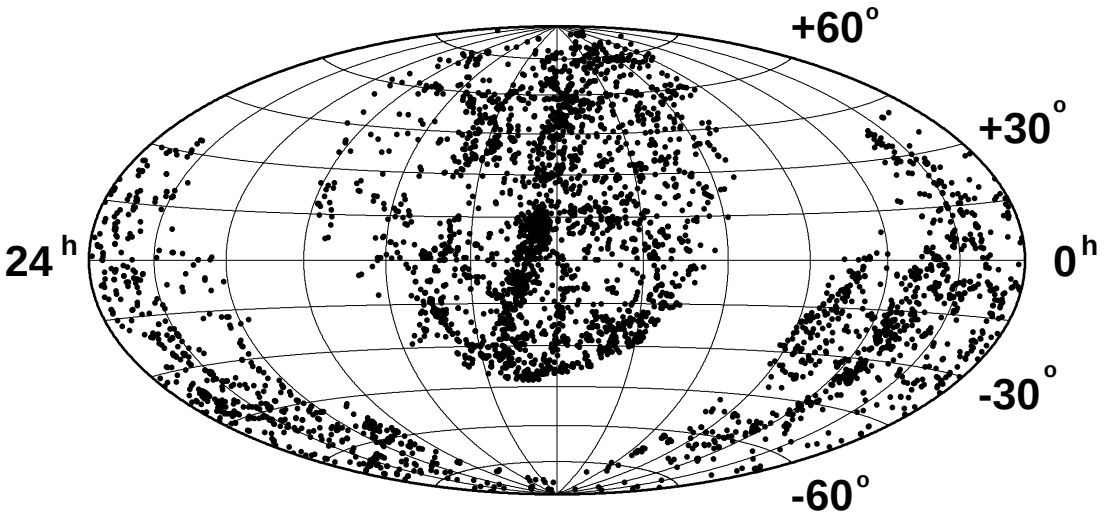

Fig. 5.— Angular distribution of galaxies in ORS data within 40Mpc in equatorial coordinate. It is noted that this database does not contain any data within $|b| \leq 20°$.

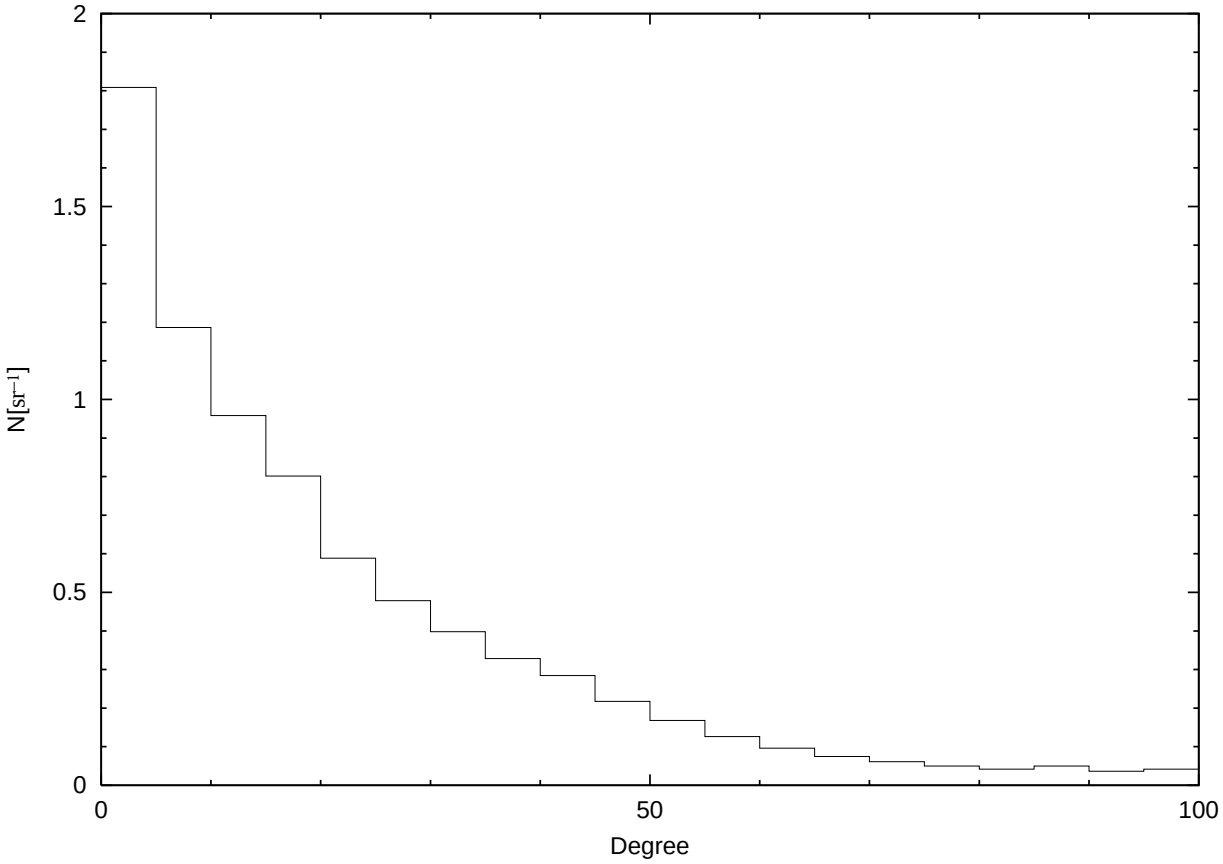

Fig. 6.— Distribution of the neighbor event (sr^{-1}) as a function of the separation angle between the two events whose energies are above 4×10^{19} eV. The number of events in a data sample is chosen to be 47. In order to estimate the mean value of every bin, the number of data samples is set to be 1000 under the same condition ($B = 10\mathrm{nG}$ and $l_c = 1\mathrm{Mpc}$).

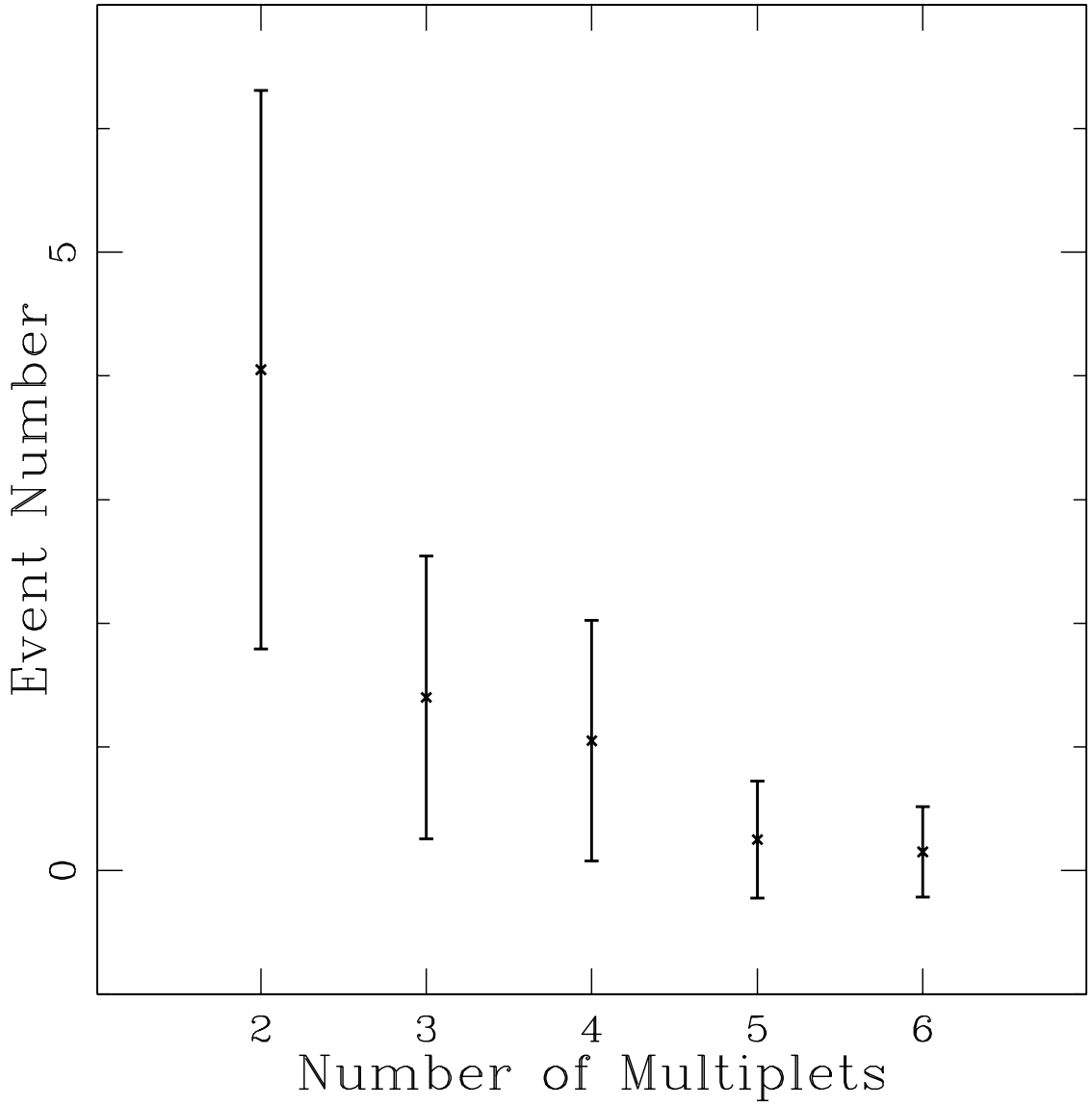

Fig. 7.— Number of clusters such as doublets and triplets within a separation angle of 2.5° in a data sample which contains 47 events, whose energies are above 4×10^{19} eV. The number of data samples is set to be 20 in order to obtain the mean values.

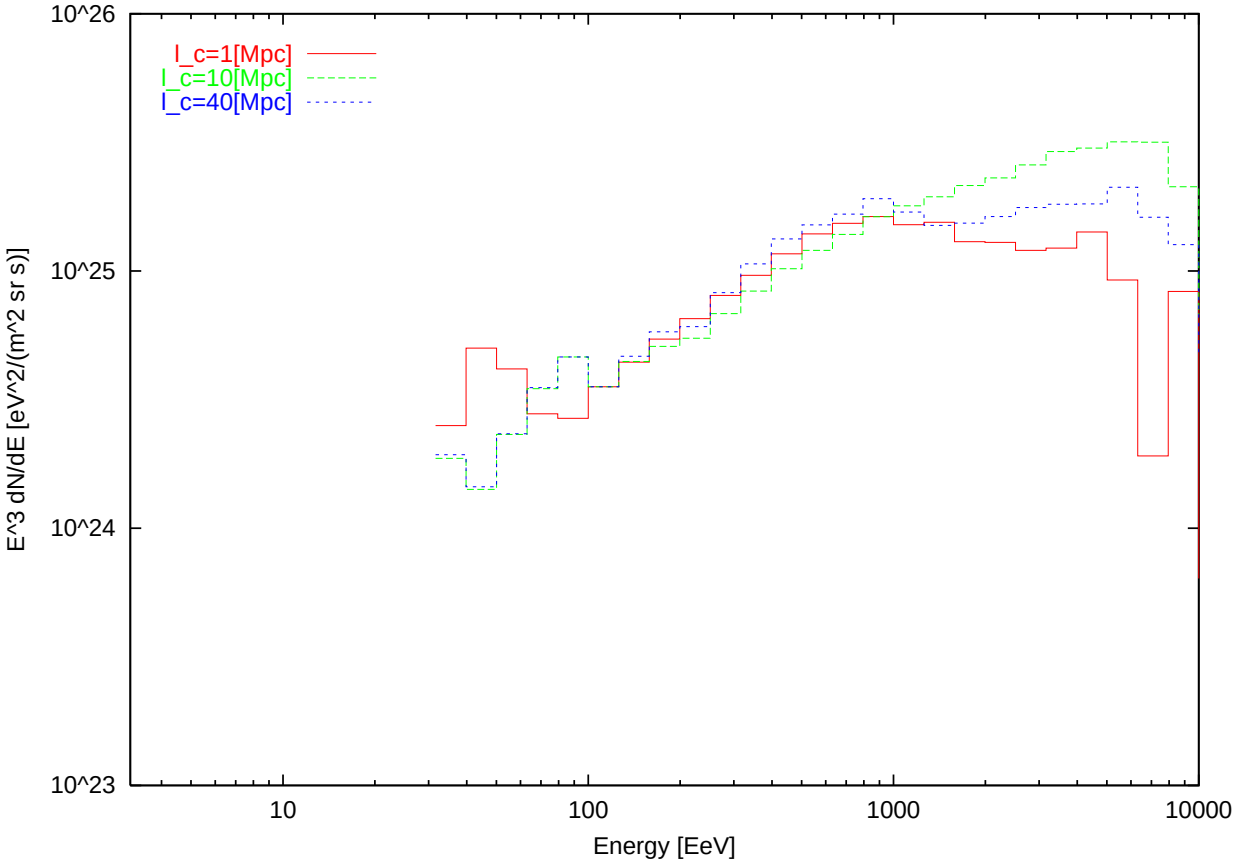

Fig. 8.— Calculated energy spectra of UHECRs. The parameters are set to be $B = 10$ nG and $H_0 = 75$ km/s/Mpc. The cases of $l_c = 1$, 10 and 40 Mpc are shown respectively. The energy spectra are normalized to the AGASA data (Hayashida et al. 1999) at $E = 100$ EeV.

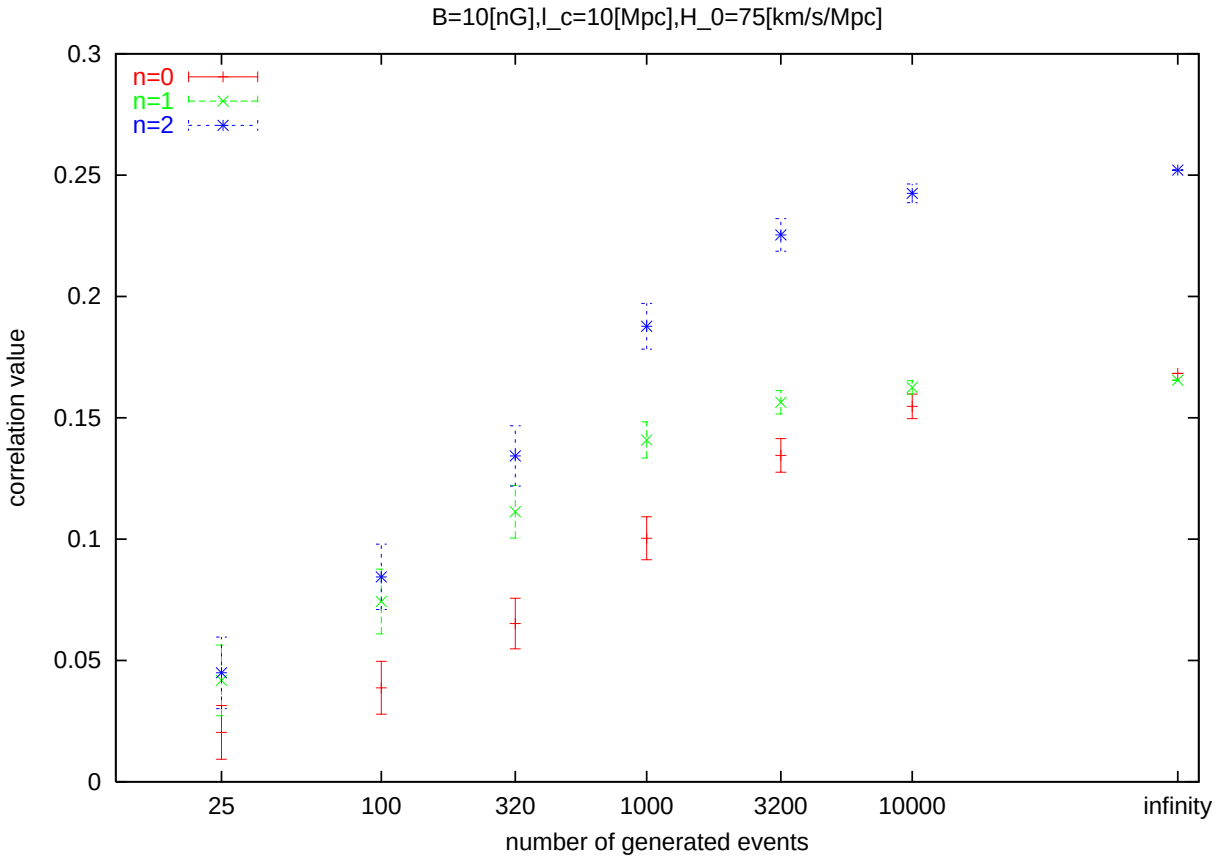

Fig. 9.— Correlation values for the case of $B = 10$ nG, $l_c = 10$ Mpc and $H_0 = 75.0$ km/s/Mpc indicating the influence of the selected energy range. $n = 0$, $n = 1$, and $n = 2$ denote $E \geq 10^{19.5}$eV, $E \geq 10^{20.0}$eV, and $E \geq 10^{21.0}$eV, respectively. It is noted that the present observed number (N) of UHECRs of order 10^1 is too small to estimate the final correlation values. When N is close to the order of 10^3 – 10^4, the correlation values begin to converge.

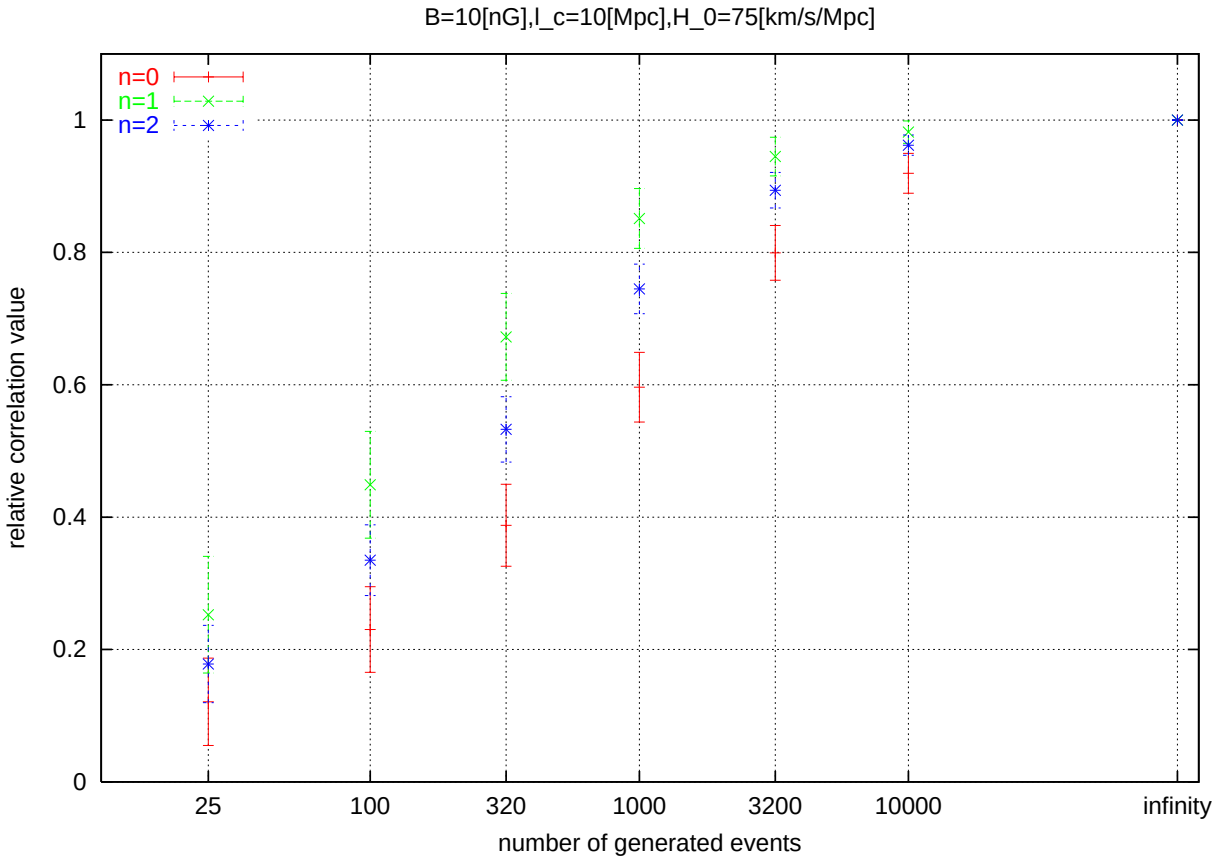

Fig. 10.— Normalized Ξ by its final value. The adopted parameters are same with Figure 9.

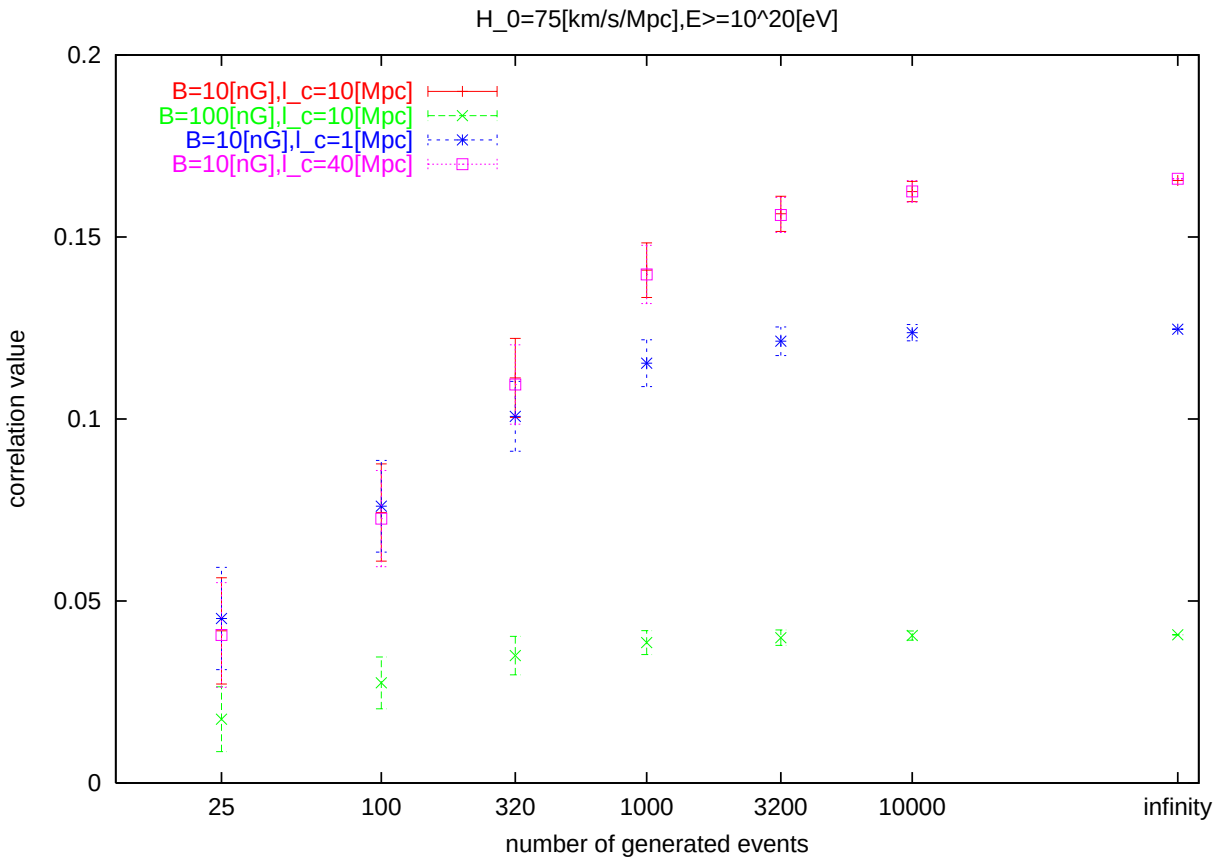

Fig. 11.— Correlation values in the case of $H_0 = 75$ km/s/Mpc and $E \geq 10^{20}$ eV indicating the influence of B and l_c. It is confirmed that the influence of B is greater than l_c.

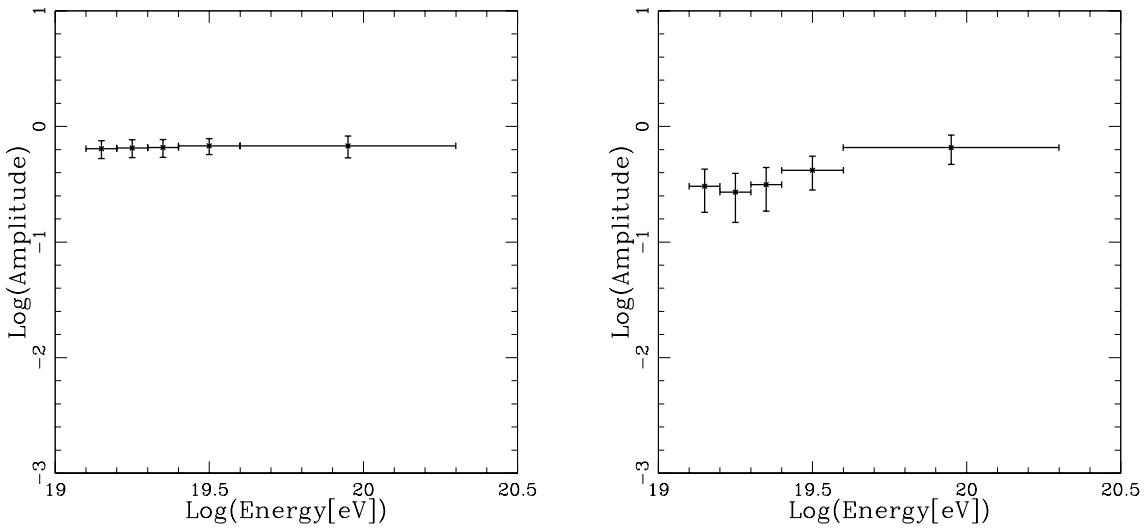

Fig. 12.— (a) left panel: amplitude of the first harmonics in galactic longitude in each energy bin for the case of $B = 10$nG and $l_c = 1$Mpc. N is chosen to be 47 in the energy range (4×10^{19} – 2×10^{20} eV) in order to compare our results with the AGASA data (Hayashida 1999). The number of data samples is set to be 1000 in order to obtain the mean value and the standard deviation in every bin. (b) right panel: same with Figure 12a, but for the second harmonics.

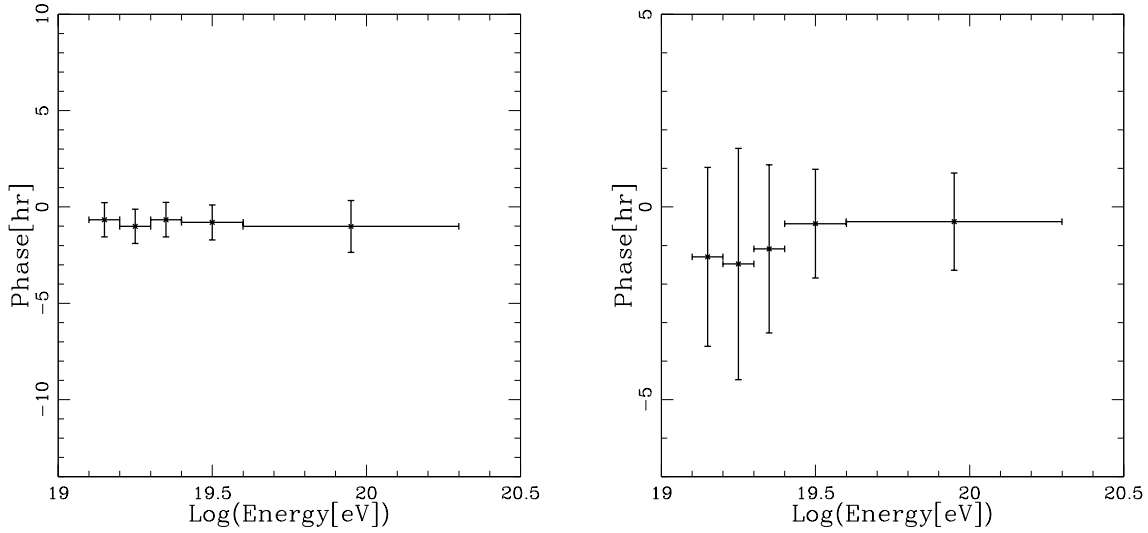

Fig. 13.— (a) left panel: same with Figure 12a, but for the phase of the first harmonics. (b) right panel: same with Figure 13a, but for the second harmonics.

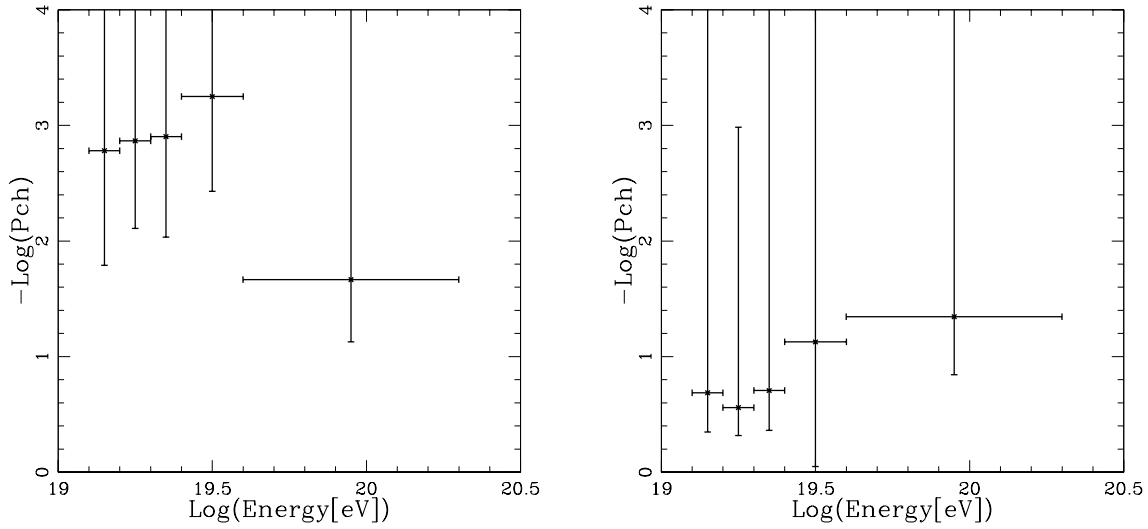

Fig. 14.— (a) left panel: same with Figure 12a, but for the chance probability of the first harmonics. (b) right panel: same with Figure 14a, but for the second harmonics.